

Methodology and some results of study of smokes in a Big aerosol chamber

R.F. Rakhimov, E.V. Makienko, V.S. Kozlov,
M.V. Panchenko, and V.P. Shmargunov

*Institute of Atmospheric Optics,
Siberian Branch of the Russian Academy of Sciences, Tomsk*

Received December 22, 2006

Some aspects of a technique for carrying out and interpretation of smoke experiment results in the Big aerosol chamber are discussed. The experiments have shown that despite sufficiently stable conditions for development of smokes in the chamber, the smoke microstructure undergoes essential qualitative and quantitative variations. A closed numerical experiment has shown that the adequate interpretation of the spectral nephelometric data strongly depends on the accuracy in preestimated mean-effective complex index of refraction of smoke particles. Analysis of some results allows an assumption that the used method gives an adequate estimate of the efficient index of refraction and particle size spectrum in the presence of a random instrumental error not exceeding 10–14%. Estimates of efficient values of the index of refraction show that there can be both weekly absorbing particles and particles close to soot by their characteristics. In the dynamics of the smoke particle characteristic sizes, there appear different trends at different intervals of size scale, which are due to appearance of different proportions in the content of particles of the intermediately dispersed fraction.

Introduction

Analysis of the microstructural changes of smoke aerosol was carried out earlier^{1–3} based on laboratory experiments in the Small aerosol chamber of 100 l volume. It was revealed that, at relatively small chamber volume for smoke particle accumulation, the efficiency of the sedimentation process (sink) of aerosols on the chamber walls, surface of tubes, transporting the disperse mixture to the measurement chamber of the nephelometer, prevails over the efficiency of other factors of the microstructural changes. Hence, the cycles of spectral nephelometric measurements were short (~ 2–3 hours). It was impossible to follow the subsequences of longer processes in the disperse mixture because of the limited sensitivity of the optical device.

In this paper, microstructural variations of smokes were studied in the Big aerosol chamber with a closed volume of 1800 m³. This allowed us to noticeably increase the duration of measurements (up to ~ 70 hours) and to extent the list of the considered factors affecting the character of microstructural variations of smokes.

The mechanisms were considered during the experiments of smoke generation at different regimes of thermal decomposition of wooden materials. The specific character of their decomposition in the regime of combustion (with appearance of flame at free access of oxygen) and pyrolysis was studied. Microstructural variations of smokes at variations of the mass of burnt samples and the temperature of decomposition were considered. The increase of duration of the observed processes, inhomogeneous

filling of the big volume of the aerosol chamber with the products of burning required the studying of some peculiarities of the methodology of the laboratory experiment statement. In this paper we consider additions to the methodology of organization of laboratory and closed numerical experiments at analysis of the measurements.

Method of the study

The results of measurements of the polarized components of the directed scattering coefficient of wood smokes $\beta_s^0(\lambda)$ under controllable conditions by means of polarization spectral nephelometer at nine wavelengths in range 0.44–0.69 μm at the angles θ of 15; 45; 110; 135; and 165° were used as initial data for optical diagnostics of microstructural variations.

Thus, 90 values of polarized components of the directed scattering coefficient (DSC) were successively measured in the experiment, which were then used in solving the inverse problem. Measurements were carried out automatically. Recording the light scattering parameters was controlled by computer on the basis of the developed algorithm with file-by-file storage of the optical data of different experiments. The full cycle of measuring DSC as a function of scattering angle and wavelength lasted for 8–9 minutes. This required the preliminary smoothing and matching of the measured data. To do this, temporal series of measured values $\beta_s^0(\lambda)$ at individual angles and wavelengths were approximated by polynomials (on linear or logarithmic scale, depending on the rate of microstructural variations), and the optical characteristics measured at different moments were reduced to a single moment.

The used approach allowed us to decrease the error in optical parameters measured at different moments, to smooth fluctuations of optical signals appearing due to spatial inhomogeneity of the smoke aerosol distribution (at small diffusion coefficients), as well as to decrease electronic noise on the measurement path. Thus, microstructural parameters were estimated with some volume averaging.

Low flow rate of transportation of the disperse mixture into the nephelometer chamber was used in the experiments, so the volume of spatial averaging coincided in practice with the volume of the nephelometer chamber (~ 5 l).

At final stages of the experiments (at small densities of the disperse mixture), the applied technique allowed us to minimize the effect of different noises of the measurement path (high-sensitive photomultiplying tubes PMT-84-3).

An example of temporal scan of $\beta_s^0(\lambda)$ values and the corresponding model approximations by polynomial of the sixth order (marked by circles) are shown in Fig. 1.

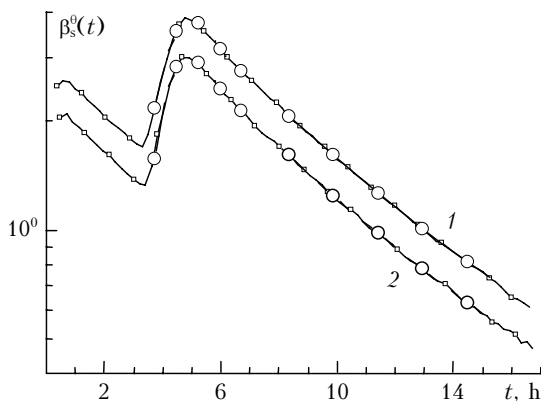


Fig. 1. Temporal series of the of spectral nephelometer signals at a scattering angle of $\theta = 110^\circ$ measured at $\lambda = 0.53$ (curve 1) and $0.69 \mu\text{m}$ (curve 2). Circles show the matching points, squares show the moments of signal recording. (Twice loading of the muffle stove by wooden samples).

Irregularity in variations of the experimental data appeared due to the necessity of double loading of the muffle stove by wooden samples, the total mass of which was 2 kg.

To estimate possible noises of the measurement path, as well as the characteristic level of the optical signals in the absence of smokes, the preliminary experiment was carried out. Long-term (10 hours and more) measurements of signals were conducted during this experiment at sampling the disperse mixture from the atmosphere at free access and through a set of aerosol filters (AFA HP) providing for effective collection of aerosols of the size more than 10 nm. Thus, we could study possible noises in detection of the optical signals and the spectral nephelometer chamber background. The results are shown in Fig. 2.

The experiments in the Big aerosol chamber have shown that the usual level of the optical signals

detected (at angles θ of $\approx 110\text{--}135^\circ$) at the final stages of settling smokes corresponds to values of the directed scattering coefficient $\sim 0.04\text{--}0.08 \text{ km}^{-1}$, which approaches the level of the signals (see Fig. 2). Actually, to solve the inverse problem, the nephelometer sensitivity allows using the optical signals measured during time series no shorter than $\sim 60\text{--}70$ h beginning from the start of the pyrolysis. Some increase in duration of experiments is possible because of increasing initial mass of the burnt wooden samples.

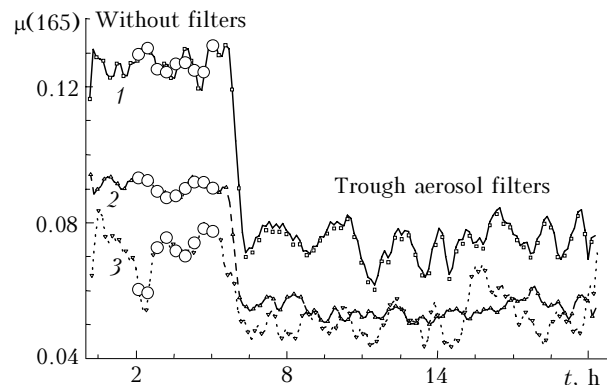


Fig. 2. The temporal series of spectral nephelometer background signals $\mu(\theta)$ at scattering angle $\theta = 165^\circ$ using aerosol filters and without them. The signals are measured at $\lambda = 0.44$, 0.50 , and $0.63 \mu\text{m}$ (curves 1–3, respectively). Circles show the matching points.

Thus, noises of the measurement path remain negligibly small as compared to the absolute value of the recorded signal of aerosol light scattering in the above time intervals, hence, the latter can be used for analysis of the smoke microstructure changes based on the inverse problem methods.

The experimental results show that the efficiency of generation of smoke particles by the used muffle stove is sufficient for homogeneous filling the aerosol chamber with the disperse mixture for 1–2 h. The greatest discrepancy between the signals recorded at different angles and wavelengths, as well as the polarized components of the scattered radiation are observed at this stage of measurements because of inhomogeneity of the chamber spatial filling. The instability of the medium under study in this period of measurements leads to a stronger dependence of the inverse problem solution on the efficiency of the matching technique and the degree of preliminary smoothing of the measurement results. Increasing degree of smoothing leads to the increase of the disperse mixture volume, over which the optical characteristics of smoke are averaged.

The homogeneity of filling the aerosol chamber with smoke increases at the next stages of the experiment, and the recorded signals show more and more coordinated and relatively smooth dynamics of temporal variations. Some peculiarities of data matching were observed in the analysis of experiments, in which subsequences of mixing the smokes of different generation regimes were considered.

Technique of the closed numerical simulation

The use of the developed approach and methods for solving the inverse problem in the framework of the closed numerical experiment shows² that the efficiency of the spectral nephelometric data interpretation essentially depends on the accuracy of preliminary estimate of the mean effective complex refractive index (CRI) of smoke particles. The deficiency of *a priori* data on the refractive index requires preliminary numerical calculations of the aerosol light scattering parameters. Earlier¹ we used the data of direct numerical simulation of aerosol light scattering parameters for preliminary analysis of spectral nephelometric measurements of smoke optical properties in the experiments in the Small aerosol chamber. Comparison of the vicinity of variations of the parameters characterizing the shape of the polarized scattering phase function (the degree of its asymmetry)⁴ with the results of model estimation helped us in some cases to estimate the vicinity of variation of the mean effective CRI value of smoke particles.

Therefore, before retrieving the size spectrum of smoke particles from the spectral nephelometric data, a series of numerical experiments were carried out in order to more precisely determine the geometrical place of points determining the parameters of the smoke scattering phase function asymmetry. The vicinity of variations of the CRI values was revealed from these data. Since both the direct simulation of aerosol light scattering parameters and solving the inverse problem were used for this purpose, these numerical estimates, in general, form the closed numerical experiment. The results of direct numerical simulation were used as initial points for estimation of CRI based on finding the minimum of the Tikhonov smoothing functional,⁵ which, as applied to the considered inverse problem, was written in the form (1) presented below. The method of finding parameters of aerosol microstructure and the refractive index of particles from the data of comprehensive optical experiments was described in detail in Ref. 6. Some results of its application to the study of smoke aerosols based on the data of polarization spectral nephelometry are presented in Refs. 2, 3, and 7.

To determine the function

$$s(r) = \pi r^2 n(r) [\mu\text{m}/\text{cm}^3],$$

where $n(r) = dN/dr$ is the number concentration of size distribution density ($\mu\text{m}^{-1}/\text{cm}^3$), the regularizing algorithm was applied based on approximation of the sought function by some step histogram $s^*(r)$.⁶ The function $s^*(r)$ was determined based on minimization of the smoothing functional:

$$F_\alpha = \sum_i^5 \eta_i \sum_j^9 \left(\sum_l^k q_{jl} S_l - q_j \right)^2 +$$

$$+ \alpha \left[p_0 \sum_l^k S_l^2 + p_1 \sum_l^{k-1} (\Delta S_{l+1,l})^2 \right], \quad (1)$$

where p_0 and p_1 are the scale coefficients; α is the parameter of regularization; $\{q_{j,l}\}$ are elements of the matrix calculated from the values of the light scattering efficiency factor $K(r,\lambda)$ for the specific particle size and scattering angle θ_k ; η_i are the weight factors, regulating the relative significance of the used spectral dependences at different scattering angles. Components of the vector of S_l solution represent the total geometric cross section of particles in the intervals Δ_l with the boundaries r'_l and r''_{l+1} . The mean value of the step function $s^*(r)$ in the above interval is determined by the ratio S_l/Δ_l .

The technique of the direct numerical simulation was based on results of the numerical experiments, in which variations of parameters of disperse mixture microstructures were determined from

$$n(r) = \frac{dN}{dr} = Ar^{-3} \sum_{i=1}^l M_i \exp \left\{ -b_i \left[\ln \frac{r}{r_{i0}} \right]^2 \right\}. \quad (2)$$

Actually, the values of the mean effective refractive index (averaged over the analyzed size range of the polydispersion ensemble of particles) were estimated for each realization of the laboratory experiment based on preliminary solution of the inverse problem taking into account the results of direct numerical simulation. This allowed us, when appearing smokes with complicated inhomogeneous microstructure, to compare the obtained results of spectral nephelometric measurements with the results of numerical simulation; to study a number of hypotheses on possible microphysical smoke peculiarities revealed from the results of measurements of polarization characteristics in special experiments. For example, possible ways of variations of CRI in the particle size spectrum were preliminary studied in some situations in the framework of closed numerical experiments, as well as the appearance of particles with inhomogeneous dielectric structure in the scattering volume (two or three layers), and the degree of the effect of random errors in optical measurements.

As an example, Figure 3 shows the results of the closed numerical experiment, in which a possibility was studied of retrieving the size spectrum and the refractive index of particles of a binary disperse mixture in the presence of different random errors in measuring spectral nephelometric data.

The results of direct numerical simulation of the aerosol light scattering parameters $\beta_s^q(\lambda)$ in the aforementioned ranges of wavelengths and scattering angles were used for solving the inverse problem. The particle size spectrum of the model medium was determined from Eq. (1), but calculations were carried out assuming that the disperse composition was formed as a binary mixture of particles, for which two CRI values were used. Particles with $r < 0.3 \mu\text{m}$ were assumed strongly absorbing (black carbon with $m = 1.84 - 0.79i$), while the particles with $r > 0.3 \mu\text{m}$

had a moderate absorption ($m = 1.54 - 0.05i$). In fact, the mixture of black carbon particles and resinous compounds in the composition of not only some individual particle, but the disperse mixture as a whole, was considered in direct simulation.

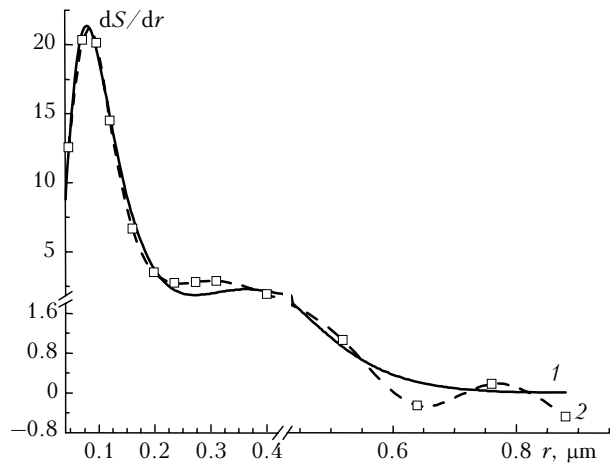


Fig. 3. Results of closed numerical experiment on retrieval of the particle size spectrum of binary disperse mixture: initial spectrum (1), retrieved spectrum (2).

Numerical experiments have shown that the random error in spectral nephelometric measurements does not exceed 10–14% for satisfactory retrieval of the particle size spectrum and determination of the complex refractive index, different in two size ranges. At such level of errors, one can determine the vicinity of the possible values of the complex refractive index and the boundary between different fractions.

Results

The conducted cycle of laboratory experiments in the Big aerosol chamber (more than 50 realizations) allowed us to develop the technique for calibration of the measurement path and to obtain a significant amount of experimental data for analysis of size spectrum transformation dynamics of smoke formations, to estimate the range of variations of CRI, and possible factors of variations of both real and imaginary parts. In particular, the results of inverting the data obtained confirmed the conclusions³ about the effect of wooden material decomposition temperature on the mean effective CRI values and especially the imaginary part. Preliminary results of analysis of the experimental data have shown that both quite transparent (in smokes of pyrolysis and smoldering) and strongly absorbing particles (in smokes of combustion) close to the parameters of black carbon can be present in the composition of smokes, that is in agreement with the estimates.^{8,9}

We have considered mainly the results of analysis of the pyrolysis smoke microstructure (without entry of air to the thermal decomposition zone) for one type of wooden sample (pine). The reason for separate consideration and conclusions about the typical peculiarity and specific manner of pyrolysis smokes as

compared to other smokes served data obtained at other regimes of thermal decomposition of wooden materials. In particular, the results of inversion of the spectral nephelometric data obtained in regime of combustion have shown that the combustion smokes are essentially finer dispersed and stronger absorbing.⁹

Figure 4 shows the particle size spectra of wooden smokes retrieved from nephelometric measurements at the stage of irregular changes of their disperse composition.

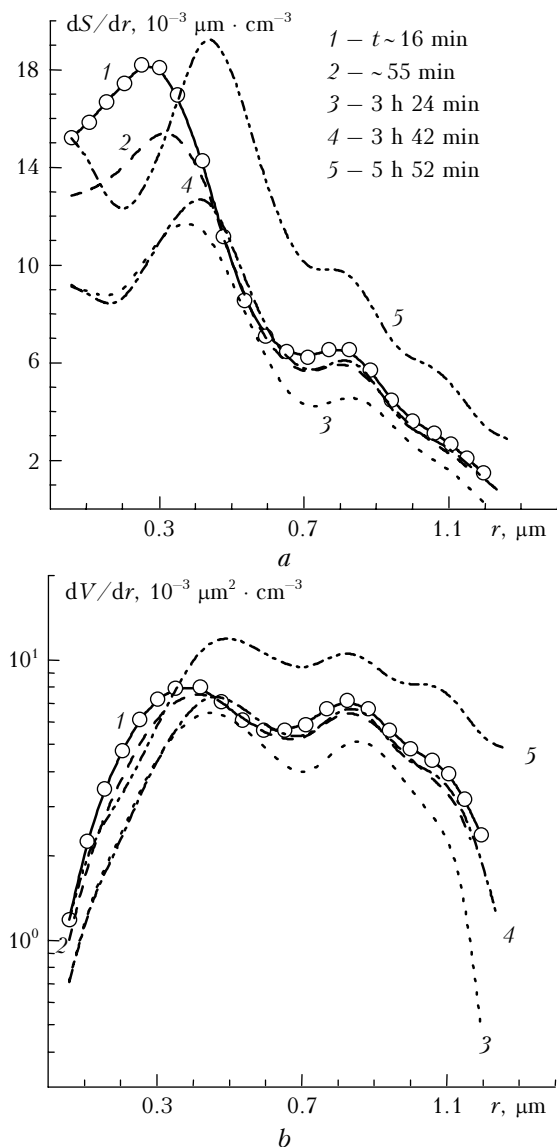


Fig. 4. The change of the smoke particle size distribution density (a) and volume (b). Twice load is used at the pyrolysis of wooden samples (pine) in the muffle stove (total mass of 2 kg).

The irregularity in variations of the optical signals in this case is caused by the fact that in the experiment the pyrolysis of wooden samples consisted of two stages, because of the limited volume of the thermal decomposition chamber in the muffle stove. Due to this fact, some increase in the aerosol particle concentration was observed at the second stage of the

experiment. On the whole, duration of the process of thermal decomposition of a 2 kg wood sample reached 5 h. Therefore, the results shown in Fig. 4 were obtained actually at the stage of filling the aerosol chamber with pyrolysis smoke and mixing smokes remaining after decomposition of the first portion of wooden samples and newly generated ones.

The data of inversion have shown that, before second loading (curves 1–3), sink of particles on the chamber walls is quite effective due to high concentration of particles, and the size spectrum, weakly changing in the shape, quite quickly loses the concentration level practically throughout all size range. Variations after the second loading are better observed in the size range of intermediately dispersed particles with $r \sim 0.4\text{--}1.3 \mu\text{m}$ (curves 4–5 in Fig. 4a). At the same time, generation of finely dispersed particles after the second loading does not lead to essential increase in their concentration. This can be explained by increasing sink of larger particles accumulated during the process of pyrolysis of the first loading. As the mass of the burnt sample increases, the optically significant mode of distribution of smoke particles widens.

According to the obtained estimates for pyrolysis smoke, the CRI values of particles averaged over the entire size range $m = 1.545 - 0.003i$ changed during the experiment with insignificant increase of both real and imaginary parts up to $1.567 - 0.005i$.

At next stages of the accumulated smoke relaxation, most effective sink of particles on the chamber walls is observed for large particles $r > 0.6 \mu\text{m}$ (Fig. 5). The effect of coagulation transformation of the size spectrum is observed from the retrieved data only at the initial stages of smoke development at their maximal concentrations and is weakly observed at the final stages, when the concentration essentially decreases. On the whole, the spectrum shape takes more indented fractional structure. Curve 1 in Fig. 5 coincides with curve 5 in Fig. 4 and corresponds to the maximal filling of the aerosol chamber with smoke particles, reached in this experiment. A stable minimum in the dynamics of the spectrum dS/dr transformation in the size range $0.22\text{--}0.32 \mu\text{m}$ should be noted (Fig. 5a), which is, possibly, related with the effective sink of particles of this size in the channels of the disperse smoke mixture transportation from the aerosol chamber to the nephelometer one. To check this hypothesis, special purpose experiments are required.

Next day of development of the smoke formation residues, the particle size spectrum takes the bimodal shape (Fig. 6) with characteristic sizes of about 0.47 and $0.85 \mu\text{m}$.

Particles with a characteristic size of $\sim 0.3\text{--}0.7 \mu\text{m}$, i.e., the first mode of intermediately dispersed particles, have the greatest optical effect at this stage of the smoke development. Our estimates have shown that the CRI values slightly decrease and reach $m \sim 1.565 - 0.004i$ at the final stages of development of pyrolysis smokes, that is a characteristic of rosin.

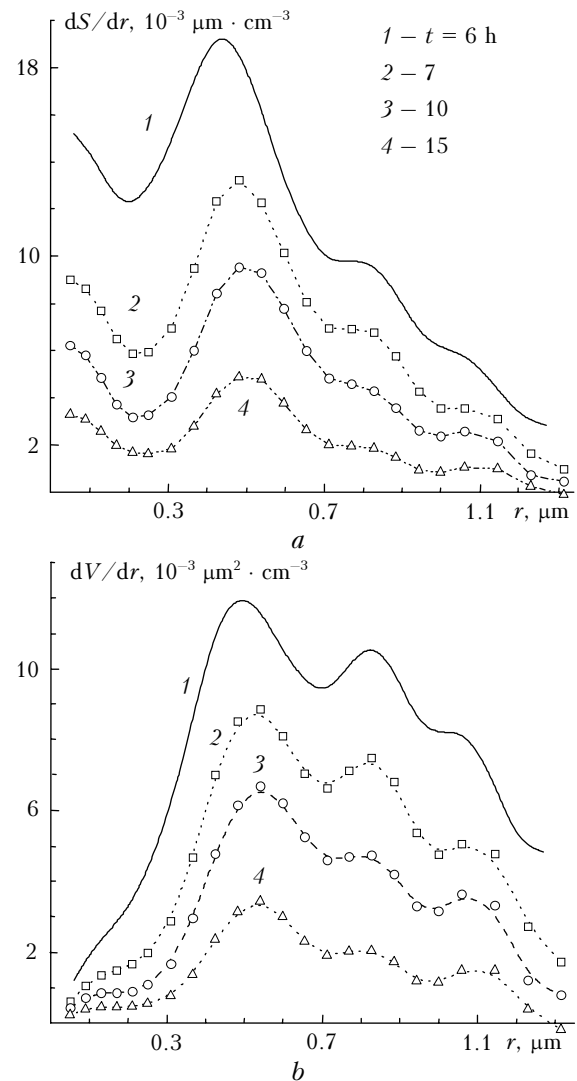


Fig. 5. Following (for Fig. 4) stages of the change of size distribution density of the total cross section (a) and volume (b); t is the time of recording the optical data (approximately ± 10 min); $m = 1.565 - 0.0058i$.

As further experiments have shown, the conclusion about stable formation of two smoke fractions holds for other pyrolysis smokes independently of the mass of burnt samples ($M \sim 0.25; 0.5; \text{ and } 1 \text{ kg}$). Note that the relative volume content of fine particles in the process of smoke settling steadily decreases. Perhaps, the noted peculiarity characterizes only the closed chamber, where the wall effect is always present. This effect in the real atmosphere will be, most likely, less pronounced, although the possibility of dry deposition of fine fraction on different elements of the rough underlying surface exists, in particular, on tree crowns in forests.

Tables 1–3 show the dynamics of the integral parameters (number density N , total geometric cross section S , and volume V) of smoke particles characteristic of different size fractions during 40 h. The values of the parameters shown in Tables 1–3 were calculated by the spectra shown in Figs. 4–6.

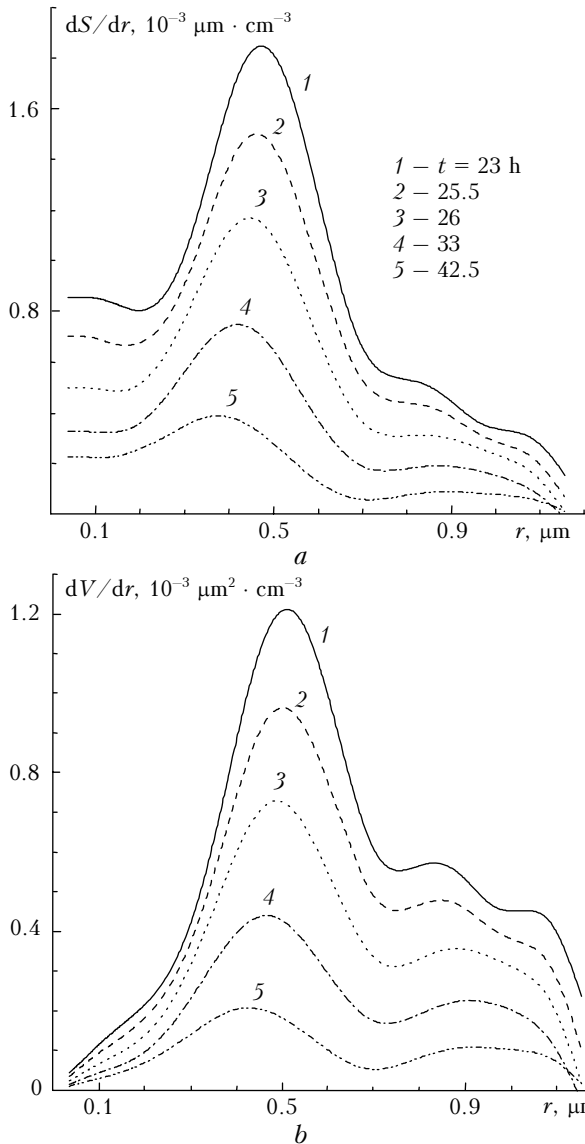


Fig. 6. Following (for Fig. 5) stages of the change of the smoke particle size distribution density of the total cross section (a) and volume (b); t is the time of recording optical data; $m = 1.565 - 0.0042i$.

Table 1. Temporal dynamics of the integral characteristics of smoke particles of $r < 0.35 \mu\text{m}$ at pyrolysis of 2 kg of pine wood

t, h	N, cm^{-3}	$S, \mu\text{m}^2 \cdot \text{cm}^{-3}$	$V, \mu\text{m}^3 \cdot \text{cm}^{-3}$	$r_{\text{ef}}, \mu\text{m}$
0.3	59288	23382	1381	0.177
0.9	57024	22296	1311	0.176
1.5	48282	19390	1155	0.179
3.0	32183	13234	798.0	0.181
3.6	31342	12970	784.6	0.181
4.7	49157	18879	1100	0.175
6.4	33830	11421	624.0	0.164
7.2	27961	10801	631.3	0.175
9.7	17851	6557.1	373.7	0.171
15.4	9710.4	3283.2	179.5	0.164
23.0	3328.0	1372.0	82.84	0.181
25.0	2727.3	1163.4	71.45	0.184
27.7	1982.7	908.02	57.78	0.191
32.6	1298.2	623.87	40.67	0.196
41.5	927.85	416.79	26.27	0.189

Table 2. Temporal dynamics of the integral characteristics of smoke particles of $0.35 < r < 0.75 \mu\text{m}$

t, h	N, cm^{-3}	$S, \mu\text{m}^2 \cdot \text{cm}^{-3}$	$V, \mu\text{m}^3 \cdot \text{cm}^{-3}$	$r_{\text{ef}}, \mu\text{m}$
0.3	5702.7	15387.3	2376.7	0.463
0.9	5647.7	15268.8	2360.8	0.464
1.5	5488.9	14807.4	2286.9	0.463
3.0	4684.6	12677.5	1961.1	0.464
3.6	5286.2	14673.8	2298.9	0.470
4.7	8321.8	23866.5	3800.6	0.478
6.4	6125.4	18036.2	2910.2	0.484
7.2	5071.0	15705.2	2599.0	0.496
9.7	3613.1	11334.4	1887.7	0.500
15.4	1763.1	5455.25	902.32	0.496
23.0	720.28	2197.70	360.98	0.493
25.0	586.05	1773.34	290.07	0.491
27.7	451.00	1332.82	215.45	0.485
32.6	277.64	788.463	124.94	0.475
41.5	127.83	339.896	52.116	0.460

Table 3. Temporal dynamics of the integral characteristics of smoke particles of $0.75 < r < 1.3 \mu\text{m}$

t, h	N, cm^{-3}	$S, \mu\text{m}^2 \cdot \text{cm}^{-3}$	$V, \mu\text{m}^3 \cdot \text{cm}^{-3}$	$r_{\text{ef}}, \mu\text{m}$
0.3	929.3	8877.3	2580	0.872
0.9	904.4	8548.6	2471	0.867
1.5	834.8	7829.2	2255	0.864
3.0	647.4	6080.8	1752	0.865
3.6	864.9	8362.7	2445	0.877
4.7	1496	15285	4595	0.902
6.4	1069	10875	3262	0.900
7.2	998.9	10223	3075	0.902
9.7	646.9	6555.7	1962	0.898
15.4	258.2	2523.2	741.7	0.882
23.0	66.87	660.71	195.3	0.887
25.0	55.35	540.68	158.9	0.882
27.7	41.23	403.81	118.8	0.883
32.6	24.88	242.72	71.28	0.881
41.5	11.93	120.96	36.22	0.898

No less complicated dynamics is observed for the particle effective sizes of the given ranges. The results of estimation are shown in Fig. 7, which illustrates the dynamics of the smoke aerosol characteristic particle sizes of accumulative and two intermediately dispersed fractions.

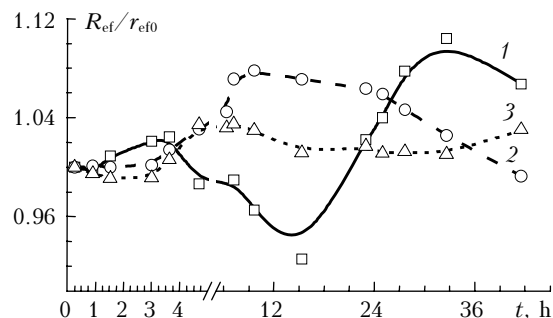


Fig. 7. Dynamics of the characteristic particle size of accumulative (1) and two intermediately dispersed (first 2 and second 3) fractions of the smoke aerosol.

Analysis of the results has shown that the second intermediately dispersed fraction of smoke aerosol takes stable size with time, and, evidently, can be

transferred in the atmosphere, weakly changing in the spectrum in the presence of other aerosol fractions. The state of particles of the fine fraction (spectrum and characteristic size) essentially depends on the concentration level of particles of intermediately dispersed range, which can favor the effective sink of fine fraction from the atmosphere.

Conclusions

The estimates of the refractive index real part of the pyrolysis smokes for pine wooden samples in the Big aerosol chamber (1800 m³), mean in the particle size range $r < 2.5 \mu\text{m}$ at different stages of thermal decomposition of samples, lie in the m range 1.5–1.6, and the imaginary part is $k < 0.005$ with high repetitiveness in numerous experiments. The obtained results correspond to the mean estimate $m = 1.55$ ($k < 0.005$) in the range $r < 0.9 \mu\text{m}$ for the pyrolysis smokes in the Small chamber (100 l) without additional humidification of air.

The estimates of the effective value of the refractive index have shown that both weakly absorbing aerosols and the particles, the properties of which approach parameters of black carbon, are present in smokes.

The efficiency of generation of smoke particles of fine fraction with $r < 0.35 \mu\text{m}$ noticeably depends on the level of the content of particles of the intermediate size $0.35 < r < 1.2 \mu\text{m}$. Thermal decomposition of the following samples of wooden materials does not lead to essential increase in the concentration of the fine fraction due to increasing efficiency of the fine particle sink and the vapors of sublimation on the surface of larger particles accumulated during the pyrolysis of wooden samples of the first loading.

The applied methodology for interpretation of spectral nephelometer data in experiments with smokes provides for a possibility of adequate estimation

of the effective refractive index and the particle size spectrum in the presence of *a priori* random measurement error not exceeding 10–14%.

Laboratory experiments have shown that, in spite of quite stable conditions of the development of smokes in the Big aerosol chamber, the smoke disperse composition undergoes essential qualitative and quantitative variations.

Acknowledgements

This work was supported in part by Russian Foundation for Basic Research (Grant No. 06–05–64842).

References

1. R.F. Rakhimov, V.S. Kozlov, M.V. Panchenko, A.G. Tumakov, and V.P. Shmargunov, *Atmos. Oceanic Opt.* **14**, No. 8, 624–628 (2001).
2. R.F. Rakhimov, V.S. Kozlov, E.V. Makienko, and V.P. Shmargunov, *Atmos. Oceanic Opt.* **15**, No. 4, 292–299 (2002).
3. R.F. Rakhimov, E.V. Makienko, M.V. Panchenko, V.S. Kozlov, and V.P. Shmargunov, *Atmos. Oceanic Opt.* **16**, No. 4, 308–317 (2003).
4. V.N. Glushko, A.I. Ivanov, G.Sh. Lifshits, and I.A. Fedulin, *Scattering of Infrared Radiation in the Cloudless Atmosphere* (Nauka, Alma-Ata, 1974), 212 pp.
5. A.N. Tikhonov and V.Ya. Arsenin, *Methods for Solving the Ill-Posed Problems* (Nauka, Moscow, 1974), 224 pp.
6. V.E. Zuev and I.E. Naats, *Inverse Problem of Lidar Sensing of the Atmosphere* (Springer-Verlag, 1983), 260 pp.
7. V.V. Veretennikov and V.S. Kozlov, in: *Study of Atmospheric Aerosol by the Method of Laser Sensing* (Nauka, Novosibirsk, 1980), pp. 186–202.
8. A.A. Isakov, *Atmos. Oceanic Opt.* **16**, No. 10, 811–816 (2003).
9. G.I. Gorchakov, P.P. Anikin, A.A. Volokh, A.S. Emilenko, A.A. Isakov, V.M. Kopeikin, T.Ya. Ponomareva, E.G. Semoutnikova, M.A. Sviridenkov, and K.A. Shukurov, *Izv. Ros. Akad. Nauk. Ser. Fiz. Atmos. i Okeana* **40**, No. 3, 366–380 (2004).